*C h a p t e r 3*

# IDENTIFYING GENES INVOLVED IN THE BIOSYNTHESIS OF MODULAR ASCAROSIDES IN *CAENORHABDITIS ELEGANS*

Panda, O.; Akagi, A.E.; Artyukhin, A.B.; Judkins, J.C.; Le, H.H.; Mahanti, P.; Cohen, S. M.; Sternberg, P.W.; Schroeder, F.C. (2017). "Biosynthesis of modular ascarosides in *C. elegans*." In: *Angewandte Chemie International Edition English* 56.17, pp. 4729-4733. doi: 10.1002/anie.201700103.

## 3.1 Abstract

*C. elegans* and other related nematodes produce a large family of small molecule signals, collectively called ascarosides, by linking together multiple building blocks derived from primary metabolic pathways. In each ascaroside, the dideoxysugar ascarylose acts as a scaffold to which different modalities are attached in a modular fashion. Although these structural differences have been shown to be responsible for the variation in behaviors regulated by individual ascarosides, the mechanisms by which specific components are linked together are unknown. We demonstrate that ACS-7, a predicted acyl-CoA synthetase that localizes in lysosome-related organelles within the intestine, is necessary for the attachment of different metabolically derived moieties to the 4'-position of the ascarylose sugar in ascr#9. Additional examination revealed that ACS-10, another putative acyl-CoA synthetase, does not appear to play a significant role in ascaroside biosynthesis.

## 3.2 Introduction

*C. elegans* and other related nematodes produce a large family of small signaling molecules known as ascarosides that control many aspects in the life of the nematode, often through conserved signaling pathways.[1-7] All ascarosides are glycosides of the dideoxysugar ascarylose with a fatty acid-like moiety attached at the 1'-position of the sugar core (Figure 3.1). The fatty acid can vary in length, level of saturation, and level of oxidation to produce different simple ascarosides (ascr). However, some ascaroside variants contain an additional head group derived from primary metabolic pathways at the 4'-position of ascarylose (Figure 3.2). For example, the indole-3-carbonyl group characteristic of icas ascarosides has previously been shown to be derived from tryptophan,[8] and the *N*-succinylated octopamine building block found attached in osas ascarosides is a product derived from tyrosine.[9] Although microorganisms are known to contain the necessary biological machinery for the synthesis of large libraries of structures, it was presumed that animals do not, and therefore the ascarosides serve as an unexpected example of structural diversity.[10-11]

Studies have shown that the small structural alterations between ascarosides are associated with substantial differences in biological function (Figure 3.3). For instance, ascr#3, the most abundantly produced ascaroside by wild type *C. elegans* hermaphrodites, is a potent male attractant and acts as a dauer formation signal. On the other hand, ascr#10 which contains a lipid side chain of equal length to that of ascr#3, but lacks a site of $\alpha,\beta$-unsaturation, attracts hermaphrodites and not males.[5, 12] Another example, icas#3, which consists of an indole-3 carbonyl attached to an ascr#3 core, acts as a hermaphrodite attractant.[8] Although the structural elements of ascarosides have known significant impacts

on worm biology, the biological machinery involved in piecing together the building blocks of ascarosides is largely unknown.

Additionally, the modular assembly of ascarosides appears to be a highly selective process. In ascr#8, the *p*-aminobenzoic terminal group attaches to the terminus of the unsaturated 7-carbon side chain of an ascr#7 core despite the fact that ascr#1 and ascr#3, which contain saturated 7-carbon and unsaturated 9-carbon side chains respectively, are more abundantly produced (Figure 3.4). This high level of specificity suggests that there may be well-regulated pathways dedicated to the biosynthesis of ascarosides. Elucidating these pathways will therefore demonstrate how the metabolic status drives the production of pheromones that regulate the behavior and development of the worm.

Using HPLC-MS analyses of the worm excretome, we found that ACS-7, a putative acyl-CoA synthetase, plays a role in the attachment of different head groups to the 4'-position of the ascarylose sugar scaffold of the simple ascaroside ascr#9. Staining and GFP-tagging studies indicate that ACS-7 localizes to the gut granules, lysosome-like organelles that are significant sites of ascaroside biosynthesis. On the other hand, ACS-10, another putative acyl-CoA synthetase, does not appear to play a role in ascaroside production.

## 3.3 Results and Discussion

### *3.3.1 Screening for Candidate Genes*

Up to this point, the only enzymes known to play a role in the production of ascarosides are those involved in the peroxisomal β-oxidation of the fatty acid side chain.[13-17] In order to identify additional genes involved in the biosynthesis of ascarosides, our collaborator, Oishika Panda in the Schroeder Lab at Cornell University, screened the

supernatant of different loss-of-function mutant worm cultures for ascaroside biosynthetic defects using HPLC-MS in comparison to a wild type control. Mutant strains were selected for testing from a collection of already available strains based on either their predicted function for creating ester bonds (Table 3.1), or their subcellular location in the peroxisomes.

Previous studies have found that samples of synthetic ascr#1 and ascr#3 fed to worms in liquid culture can be converted into their indolated derivatives icas#1 and icas#3, respectively.[13] This suggests that ascaroside modification at the 4'-position occurs after the attachment and peroxisomal β-oxidation of the fatty acid side chain. The headgroups attached to the 4'-position of ascarylose are connected by ester bonds, making genes encoding *O*-acyltransferases prime candidates as potential players in the ascaroside biosynthetic pathway.

In *C. elegans*, 61 genes are annotated as putative *O*-acyltransferases based on homology, and out-crossed knockout mutants were available readily for only three genes: *oac-39(gk149)*, *nrf-6(sa525), and ndg-4(sa529)*. To expand our examination of the *oac* family, we also studied strains obtained from the Million Mutant Project (MMP). These strains are derived from the mutagenesis of wild type animals with ethylmethanesulfonate, *N*-ethyl-*N*-nitrosourea, or a mixture of both. As such, these strains contain a large number of mutations, but we specifically selected strains containing amber, ochre, or opal stop codons within the *oac* gene sequences, which are likely to disrupt proper translation and therefore have a higher probability of disrupting enzyme function.[18] As truncation of the fatty acid side chain occurs in the peroxisomes, we also selected genes containing peroxisome targeting sequences including three putative acyl-CoA synthetase genes from the *acs* gene family.[19]

From the initial LC-MS screen, four of the 19 MMP strains examined demonstrated reduced levels of mbas#3 compared to a wild type control. These strains contained mutations in *oac-14(gk519224)*, *oac-38(gk648702)*, *oac-29(gk646323)*, and *oac-50(gk402144)*. The potent aggregation pheromone mbas#3 is a derivative of ascr#3 and contains a tiglic acid moiety on the 4'-position of the ascarylose sugar.

Although all four *oac* mutant strains produced decreased levels of mbas#3, levels of the precursor ascaroside ascr#3 were similar to wild type. To rule out the possibility that the lower mbas#3 levels observed were not due a decrease in tiglic acid, cultures of *oac-38(gk648702)* and *oac-50(gk402144)* mutant worms, which produced the lowest mbas#3 levels of the four strains, were supplemented with tiglic acid or an ethanol control (Figure 3.5). The results demonstrate that mbas#3 production was rescued in *oac-38(gk648702)* with the addition of tiglic acid, but not in *oac-50(gk402144)*. This suggests that *oac-50* may play a role in the biosynthesis of mbas#3, but that the change in mbas#3 production observed in the *oac-38(gk648702)* is most likely due to a change in tiglyl-CoA metabolism.

Initial HPLC-MS screening of putative peroxisomal genes revealed that the *acs-7(tm6781)* mutant is unable to produce the modular ascarosides icas#9 and osas#9, although the levels of other modular ascarosides such as icas#3, icas#10, and osas#10 were similar to wild type (Figure 3.6). This result suggests that *acs-7* may be important in the modification of the simple ascaroside ascr#9 at the 4'-position.

### *3.3.2 Examining the Role of oac-50 in Ascaroside Biosynthesis*

The MMP strain containing the *oac-50(gk402144)* mutation contains 218 additional mutations (Figure 3.7). To ensure the observed defects in mbas#3 production were

specifically due to a loss of function in *oac-50* and not another gene, the MMP strain was outcrossed three times with wild type N2 worms to eliminate background mutations. The outcrossed *oac-50(gk402144)* worms were then fed either tiglic acid or ethanol as a control to confirm that any observed reduction in mbas#3 production is due to an ascaroside biosynthetic defect caused by the *oac-50* mutation and not due to a background mutation.

Results from the feeding assay revealed that the outcrossed *oac-50* mutant strain produces mbas#3 levels similar to wild type when fed either tiglic acid or ethanol (Figure 3.8). This rescue of mbas#3 production indicates that *oac-50* does not play a role in ascaroside production. It is possible that the reduced mbas#3 phenotype previously observed is due to one of the background mutations eliminated through the outcrossing process, however which specific mutation is responsible is not immediately apparent based on the predicted functions of each gene based on homology.

### *3.3.3 Transgenic Rescue of ACS-7 Restores the Production of ascr#9 Derivatives*

The gene *acs-7* is an ortholog of human acyl-CoA synthetase bubblegum family member 1 and is therefore predicted to be an acyl-CoA synthetase; however, the specific function of the gene within *C. elegans* has not previously been identified. In order to confirm the role of ACS-7 in the biosynthesis of the modular ascarosides icas#9 and osas#9 as indicated by our initial screen, we drove the expression of a C-terminal green fluorescent protein (GFP)-tagged ACS-7 fusion protein (ACS-7::GFP) under the native *acs-7* promoter (*Pacs-7:acs-7::gfp*) within an *acs-7(tm6781)* loss-of-function mutant background.

HPLC-MS analysis of the supernatant obtained from *Pacs-7::acs-7::gfp* liquid cultures demonstrated rescue of the production of icas#9 and osas#9 (Figure 3.9). Other

ascaroside levels remained similar to wild type. Furthermore, although ascr#9 levels remained consistent amongst wild type N2, the *acs-7(tm6781)* loss-of-function mutant, and the *Pacs-7::acs-7::gfp* rescue strain, restoration of osas#9, icas#9, and tsas#9 indicate that ACS-7 is specifically involved in the biosynthesis of ascr#9 derivatives (Figure 3.10). Our collaborators went on to demonstrate through *in vitro* assays using recombinant ACS-7 protein that ACS-7 activates head groups prior to attachment to the ascarylose core by adenylating the precursors.[20] ACS-7 does not carry out the esterification, or *O*-acyltransferase, step.

### *3.3.4 The Role of LROs in Modular Ascaroside Biosynthesis*

Although the *acs-7* gene contains a peroxisomal targeting sequence (PTS) and was therefore predicted to encode a peroxisomal protein, the localization of ACS-7 had not previously been examined. Fluorescence microscopy of worms co-expressing an ACS-7::GFP fusion protein along with an mCherry fluorescent protein containing an SKL peroxisomal tag and driven under the intestine-specific promoter for the *vha-6* gene (*Pvha-6::mCherrySKL*) revealed that the ACS-7::GFP protein does not colocalize with the peroxisomal marker (Figure 3.11). Therefore, although the *acs-7* gene contains a PTS tag, the protein is not peroxisomal.

*C. elegans* is known to contain punctate, birefringent organelles in the intestine called the gut granules.[21-22] Although there are several types of gut granules, acidic lysosome-related organelles (LROs) are known to play significant roles in breaking down digestive waste, regenerating biomolecular building blocks, and are hypothesized to be involved in the biosynthesis of various metabolites.[23-24] Through staining studies using LysoTracker red, a

dye that selectively stains LROs, it was revealed that ACS-7::GFP colocalizes with the dye, indicating that ACS-7::GFP localizes in the LROs within the intestine of *C. elegans* (Figure 3.12). Our collaborators in the Schroeder Lab found that strains with mutations in genes required to produce gut granules such as *glo-1*, a member of the Rab family of small GTPases, and *pgp-2*, a member of the ABC transporter family, are unable to produce or product reduced quantities of ascarosides modified at the 4'-position, suggesting that these more complex ascarosides are synthesized specifically in the LROs (Figure 3.13).[20] Our localization data and rescue experiments for the *acs-7* gene further support this hypothesis.

### *3.3.5 Knockout of acs-10 Does Not Impact Ascaroside Biosynthesis*

As *acs-7* was shown to be involved in the biosynthesis of modified derivatives of ascr#9, we hypothesized that other members in the *acs* gene family may be involved in the production of 4'-modified versions of other simple ascarosides. There are 22 members in the *acs* gene family, all predicted to be fatty acid-CoA synthetases based on homology and orthology data; however, there are only mutant strains available from the Caenorhabditis Genetics Center for seven of the genes. We therefore utilized the CRISPR/Cas9 gene editing system to create an additional loss-of-function mutant strain for the gene *acs-10*.

The *acs-10* gene shares 30% homology to *acs-7*. We generated a mutant that contains a 1182 base pair deletion that covers the most of last two exons and a significant portion of the 3'UTR region (Figure 3.14). We predict that this is a loss-of-function deletion as it includes 16 of the 19 residues in the predicted active site and 15 of 16 residues in the predicted AMP binding site. However, HPLC-MS analysis of mutant *acs-10* liquid cultures revealed that all known ascarosides were produced at similar levels to a wild type control

(Figure 3.14). Therefore, we conclude that unlike *acs-7*, *acs-10* plays no significant role in the biosynthesis of ascarosides modified at the 4'-position.

## 3.4 Conclusions

In summary, by driving the expression of a GFP-tagged *acs-7* transgene within a mutant *acs-7* loss-of-function mutant background, we found that ACS-7 rescues the production of icas#9, osas#9, and tsas#9, and thus plays a role in the creation of ascr#9 derivatives. This also suggests that other enzymes are required to play similar roles in the biosynthesis of modular ascarosides containing different fatty acid side chains. Although loss of function in the gene *acs-10* did not demonstrate any ascaroside biosynthetic defects, we suggest conducting further screens on other mutants from the *acs* gene family.

Through colocalization and staining studies, we discovered that ACS-7 is expressed in acidic LROs. Furthermore, abolishment or reduction of gut granules resulted in a loss or reduction in the production of ascarosides modified at the 4'-position, but not the corresponding precursor simple ascarosides. These results demonstrate that *C. elegans* homologs of genes from canonical metazoan metabolic pathways act in specific organelles to create complex metabolites. In future, it may be useful to perform organelle-specific proteomics studies to identify other proteins that may be involved in the attachment of head groups to other simple ascarosides such as ascr#3 and ascr#10.

Although our initial study of an *oac-50* loss-of-function mutant failed to display any defects in ascaroside biosynthesis, the *oac* family of genes is still a prime target for screening. Our initial screen may have failed due to MMP strains containing too many mutations. Ascaroside biosynthesis is a highly regulated process that is influenced by many

environmental factors including temperature, nutrient density and population. Therefore, an additional mutation may alter ascaroside biosynthesis indirectly by influencing the worm's metabolism. We therefore suggest the creation of mutant strains containing loss-of-function mutations in single *oac* genes using the CRISPR-Cas9 genome editing system.

## 3.5 Figures

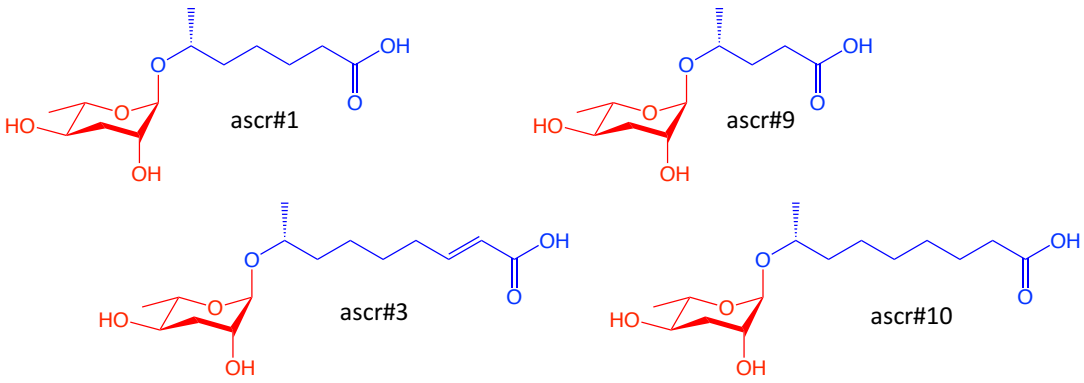


**Figure 3.1: Simple Ascaroside Structures.** The simple ascarosides ascr#1, ascr#3, ascr#9 and ascr#10 all consist of an ascarylose sugar core (red) with different fatty acid-like moieties at the 1'-position (blue).

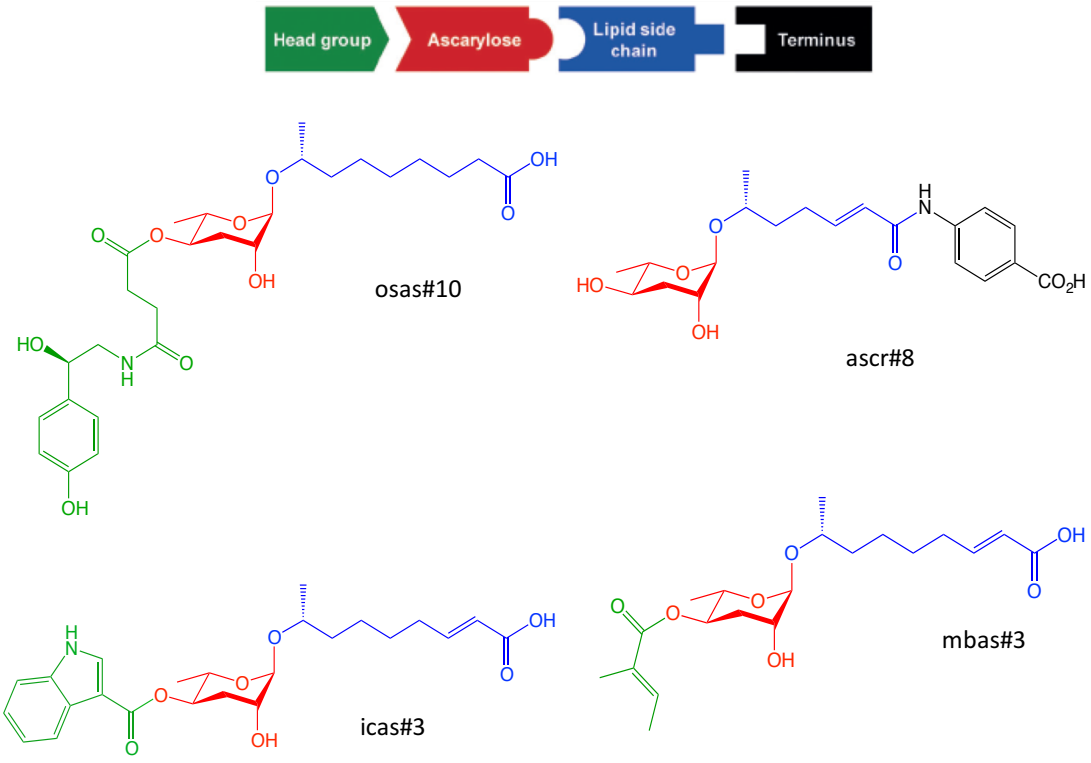


**Figure 3.2: Modular Ascaroside Structures.** Modular ascarosides consisting of a simple ascaroside core (red) with a head (green) or terminal (black) group derived from neurotransmitter (osas#10), amino acid (icas#3), fatty-acid (mbas#3), or folate (ascr#8) metabolic pathways.

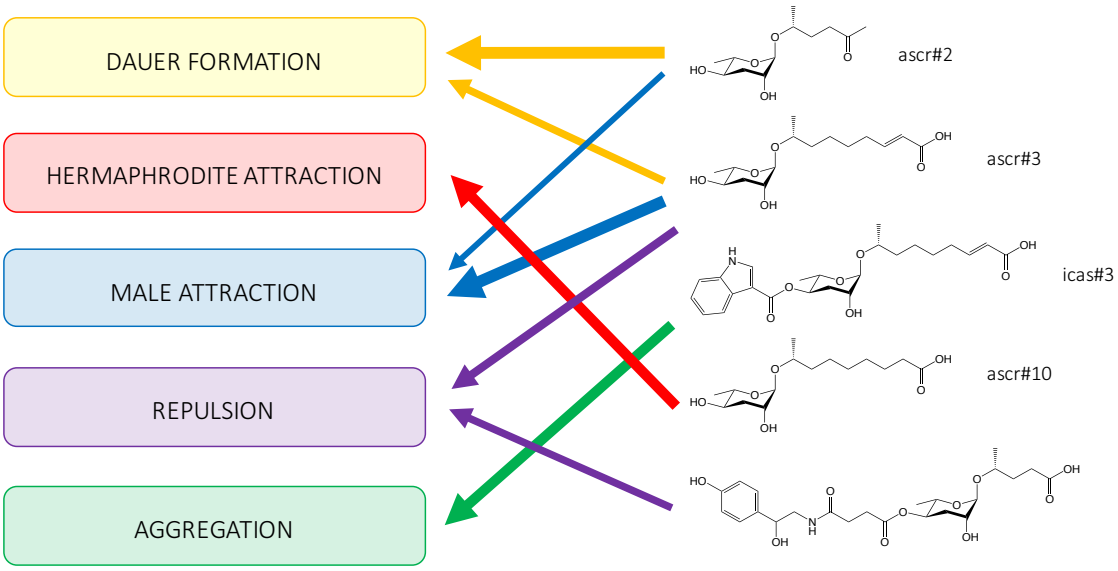


**Figure 3.3: Ascaroside Structure Determines Biological Function**. Although ascr#3 is a major component of dauer pheromone and known to attract male *C. elegans* worms, ascr#10, which has a carbon chain of similar length, but lacks a site of unsaturation, is a hermaphrodite attractant. Furthermore, when ascr#3 is modified with an indole-3-carbonyl at the 4'-position, icas#3, an aggregation pheromone, is formed. Small structural differences amongst ascarosides thus result in large differences between behaviors demonstrated by the worm. Width of arrows represent the relative potency of the ascaroside in each specific behavior.

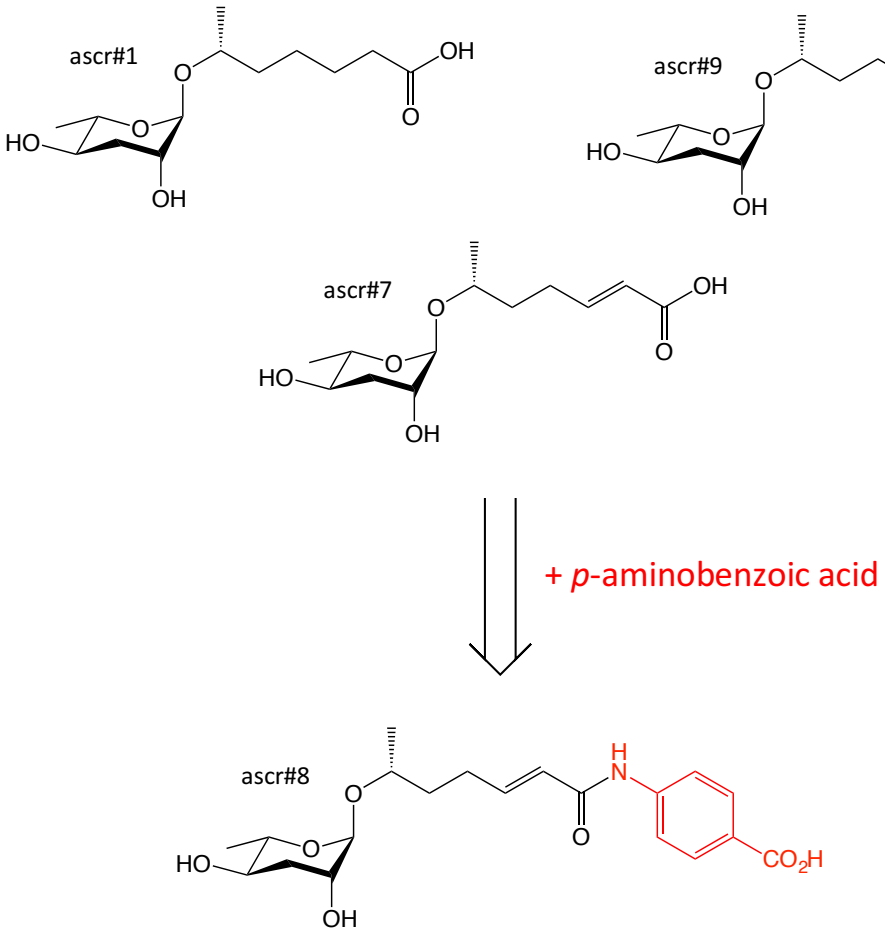


**Figure 3.4: Specificity in Ascaroside Modification.** A *p*-aminobenzoic acid group preferentially attaches to the terminal end of the lipid side chain of ascr#7 to form its derivative ascr#8, despite the fact that ascr#1 and ascr#9, which contain lipid side chains of similar length and level of saturation, respectively, are more abundantly produced.

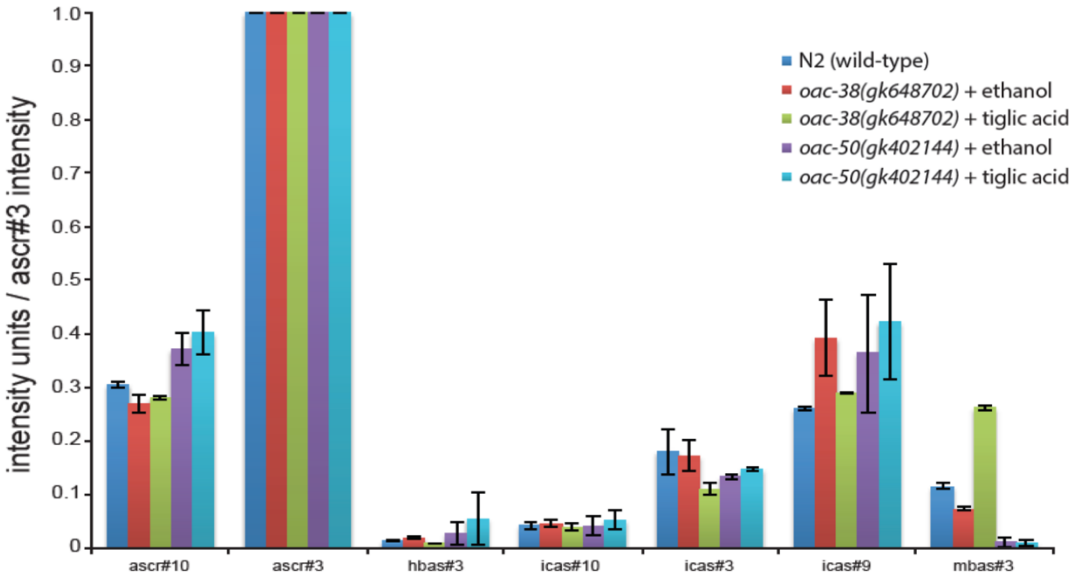


**Figure 3.5: Tiglic Acid Feeding Assay with *oac* Mutants**. Upon the addition of tiglic acid to worm cultures, mbas#3 production was rescued in the *oac-38(gk648702)* mutant, but not the *oac-50(gk402144)* mutant. Averages and standard deviations were calculated from at least two biological replicates.

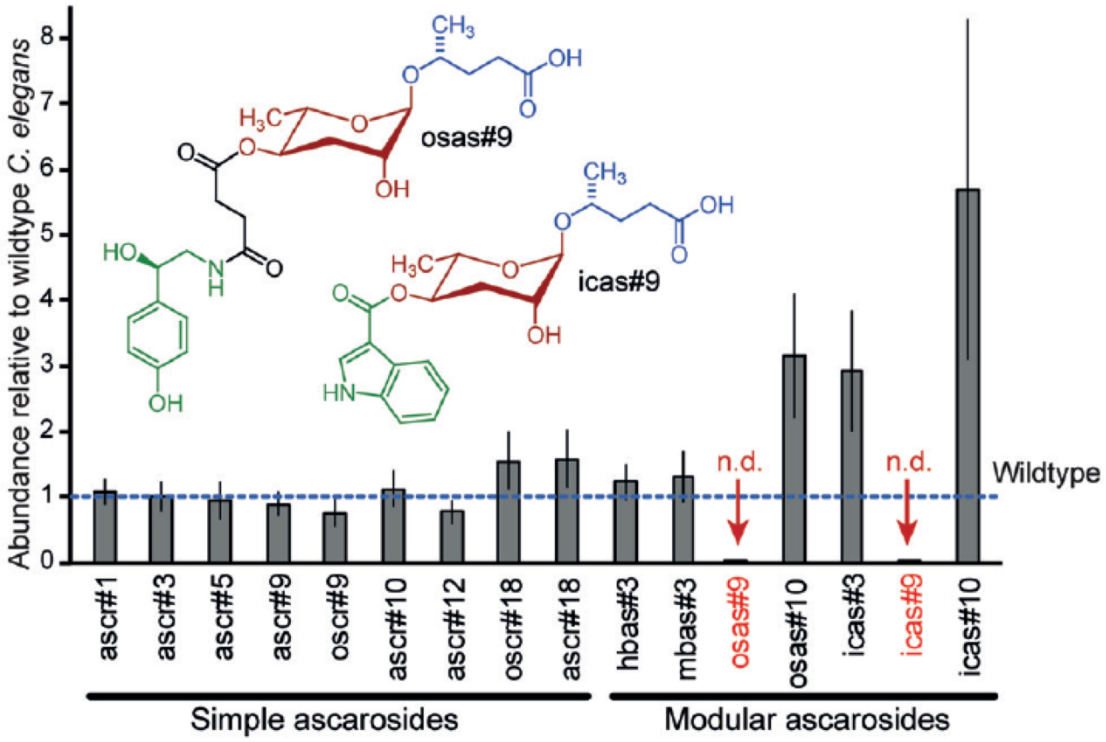


**Figure 3.6: The Mutant *acs-7(tm6781)* Lacks ascr#9 Derivatives.** A comparison of ascaroside abundance in *acs-7(tm6781)* mutants normalized to ascaroside levels produced by wild type *C. elegans* as determined by HPLC-MS analysis. The presence of icas#9 and osas#9 were not detected (n.d.). (Figure from Panda *et al*.[20])

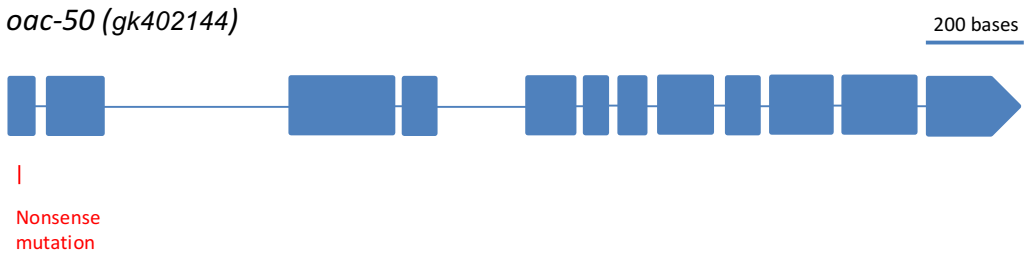


**Figure 3.7: The *oac-50(gk402144)* Mutant.** The Million Mutation strain VC20784 contained 219 mutations including the *oac-50(gk402144)* allele which contained a nonsense mutation in the first exon of the gene.

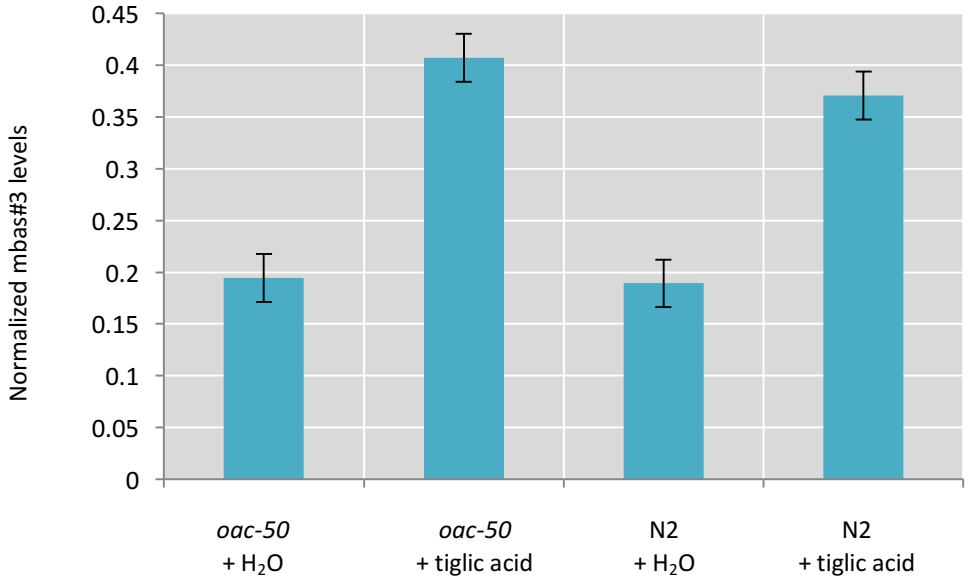


**Figure 3.8: Feeding Tiglic Acid to an Outcrossed *oac-50(-)* Mutant.** When fed tiglic acid or ethanol, the outcrossed *oac-50* mutant produced mbas#3 levels similar to N2. The levels of mbas#3 are normalized to ascr#3 levels. Error bars represent the standard deviation between three biological replicates.

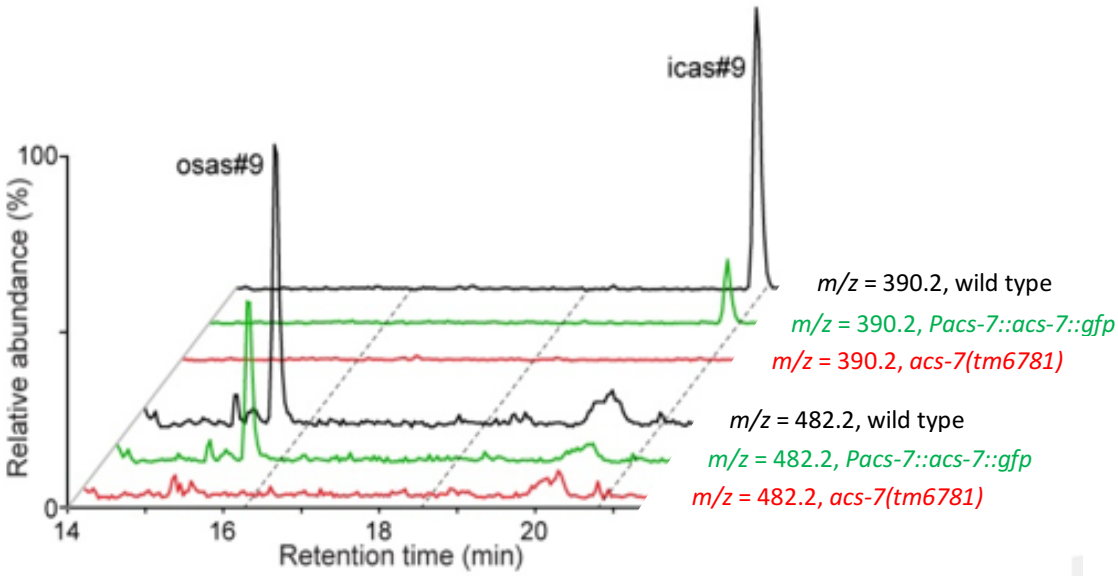


**Figure 3.9: ACS-7::GFP Rescue Restores ascr#9 Derivatives**. HPLC-MS (ESI-) ion chromatograms for icas#9 and osas#9 demonstrate rescue of icas#9 and osas#9 production in *Pacs-7::acs-7::gfp* transgenic worms (green) compared to the *acs-7(tm6781)* loss-of-function mutant (red). Wild type N2 worms (black) produce both ascr#9 derivatives. (Modified figure from Panda *et al*.[20])

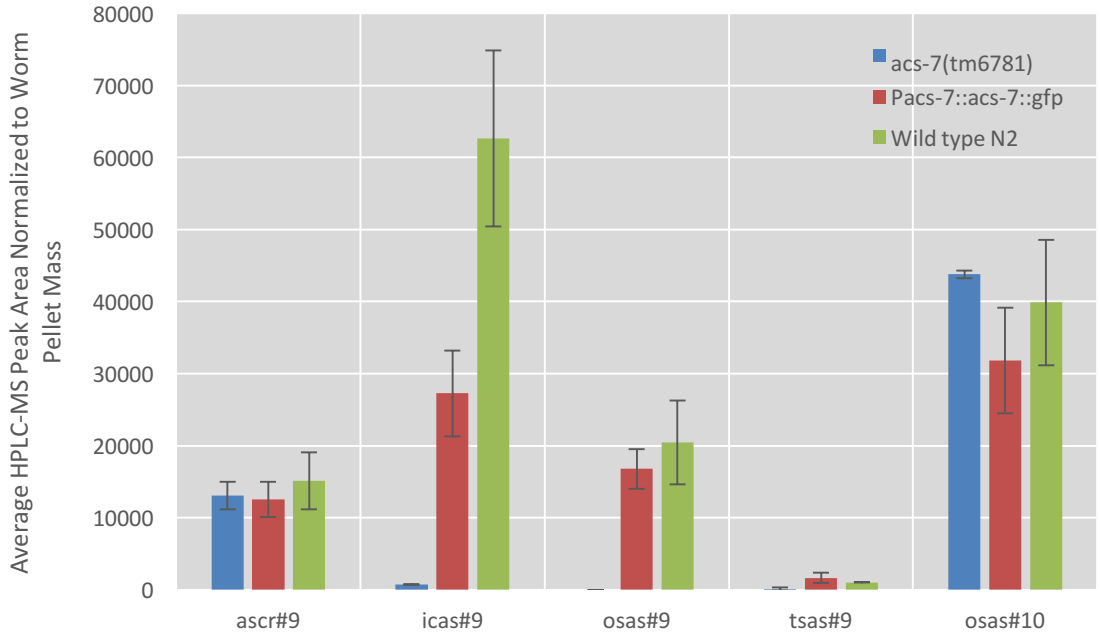


**Figure 3.10: Rescuing Production of ascr#9 Derivatives.** As determined by HPLC-MS analysis of liquid worm culture supernatant, the production of icas#9, tsas#9, and osas#9 is restored in worms expressing an ACS-7::GFP fusion protein. The levels of ascr#9 remain consistent in all three worm strains. MS peaks are normalized to worm pellet mass. Error bars represent the standard deviation between two biological replicates.

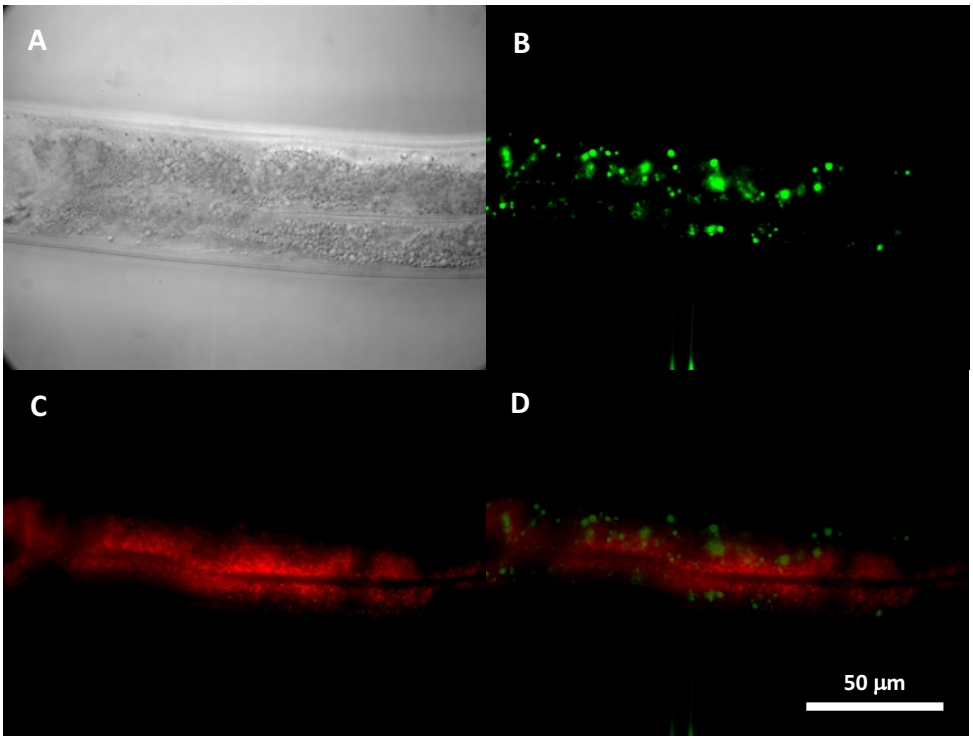


**Figure 3.11: ACS-7::GFP Does Not Localize to the Peroxisomes.** A) A DIC image of the midsection of a young adult worm expressing an ACS-7::GFP fusion protein under the *acs-7* promoter, an mCherry peroxisomal marker, and an *unc-119*(+) rescue construct within an *unc-119(-)* mutant background. B) ACS-7::GFP expression is localized to punctate organelles within the intestine. C) mCherry fluorescent protein with a peroxisomal tag is expressed under the *vha-6* intestinal promoter. D) Overlay of (B) and (C) reveal that ACS-7::GFP does not colocalize with the peroxisomal mCherry marker.

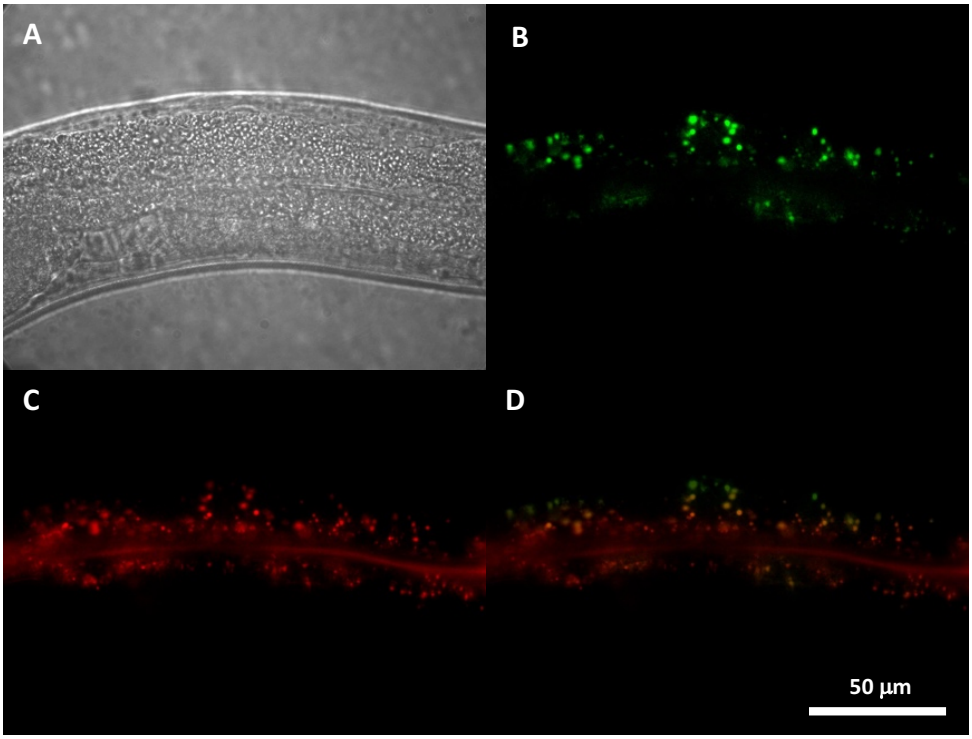


**Figure 3.12: ACS-7::GFP Localizes to the LROs.** A) A DIC image of the midsection of a young adult worm expressing ACS-7::GFP under the native *acs-7* promoter. B) ACS-7::GFP localizes to punctate organelles within the intestine. C) Staining of LROs with LysoTracker Red. D) Overlay of (B) and (C) reveal that ACS-7::GFP localizes to the LROs.

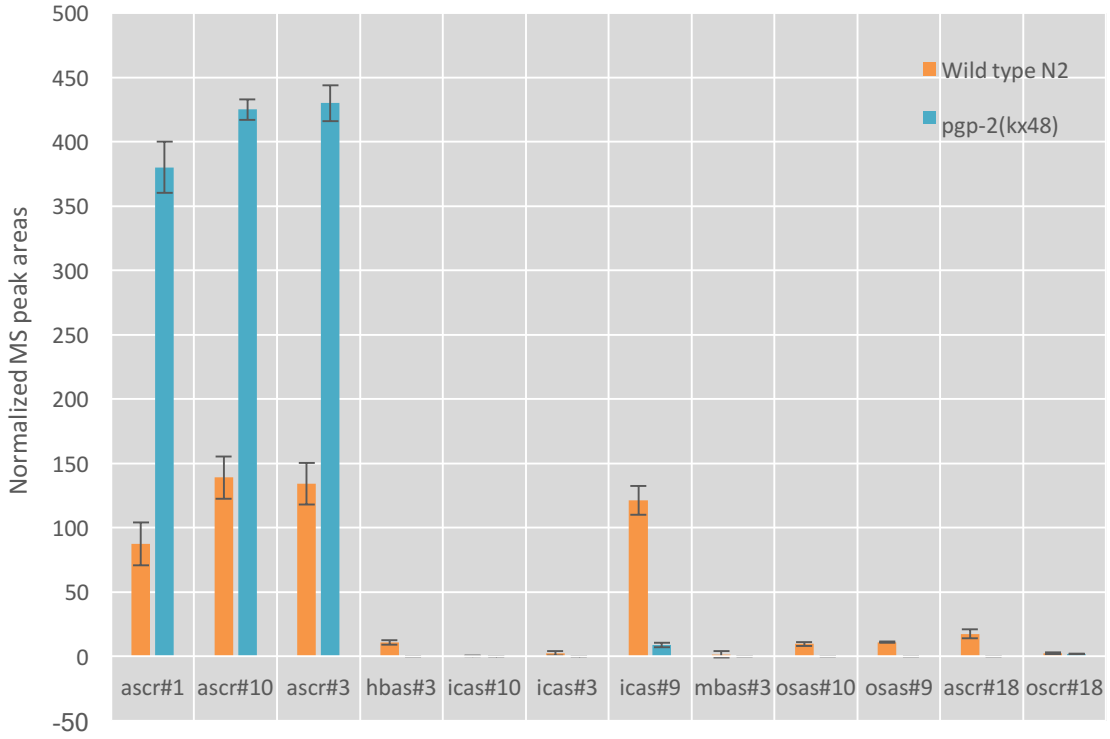


**Figure 3.13: LRO Mutants Do Not Produce 4'-Modified Ascarosides.** The gene *pgp-2* is a member of the ABC transporter family. Mutants with a loss-of-function in *pgp-2* are unable to form gut granules in the intestine. HPLC-MS analyses reveal that *pgp-2(kx48)* mutant worms do not make appreciable quantities of ascarosides modified at the 4'-position. Error bars represent the standard deviation between biological replicates.

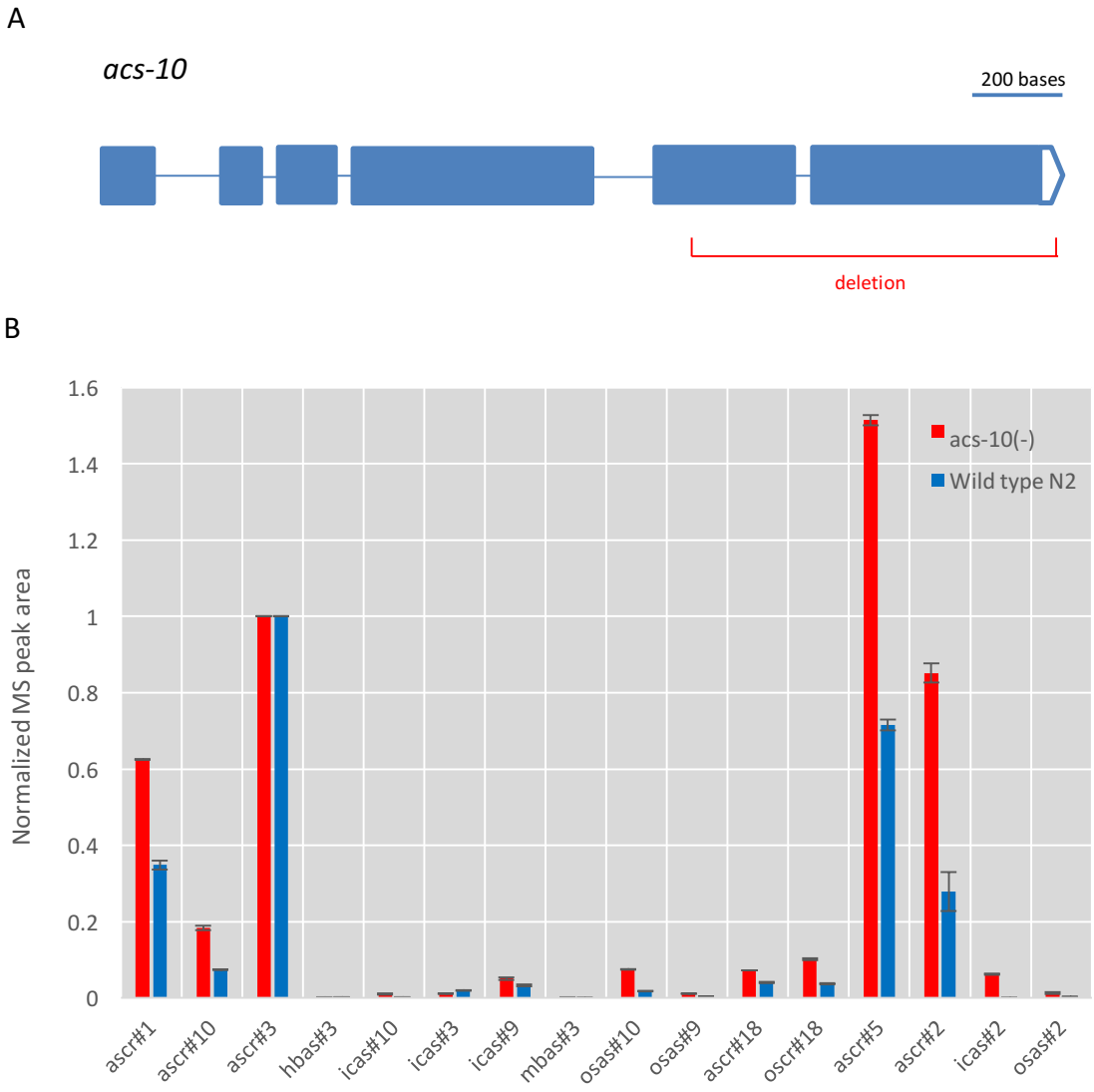


**Figure 3.14: The *acs-10* Gene Does Not Play a Role in 4'-Modification**. A) Schematic of the 1182 base pair deletion spanning the last two exons and part of the 3'UTR region of the *acs-10* gene. B) HPLC-MS analysis of an *acs-10* mutant metabolome reveals no significant difference in ascaroside production compared to a wild type control. Peak areas from HPLC-MS chromatogram are normalized to ascr#3 levels. Data represents two biological replicates for each strain. Error bars represent the standard deviation between replicates.

## 3.6 Tables

**Table 3.1** *O*-acyltransferase mutant strains screened by HPLC-MS for ascaroside biosynthetic defects.

| Gene | Strain | Source | Initial Screen Result |
|---|---|---|---|
| *ndg-4*(*sa529*) | JT529 | Deletion mutant from CGC | Wild type |
| *nrf-6*(*sa525*) | JT525 | Deletion mutant from CGC | Wild type |
| *oac-11*(*gk531381*) | VC40243 | Million Mutation Project | Wild type |
| *oac-14*(*gk519224*) | VC40217 | Million Mutation Project | Wild type |
| *oac-14*(*gk786954*) | VC40738 | Million Mutation Project | Reduced mbas#3 |
| *oac-16*(*gk914989*) | VC40988 | Million Mutation Project | Wild type |
| *oac-20*(*gk256989*) | VC10128 | Million Mutation Project | Wild type |
| *oac-23*(*gk445127*) | VC30240 | Million Mutation Project | Wild type |
| *oac-27*(*gk694121*) | VC40561 | Million Mutation Project | Wild type |
| *oac-29*(*gk646323*) | VC40455 | Million Mutation Project | Reduced mbas#3 |
| *oac-3*(*gk252641*) | VC20209 | Million Mutation Project | Wild type |
| *oac-34*(*gk652397*) | VC40469 | Million Mutation Project | Wild type |
| *oac-35*(*gk883174*) | VC40922 | Million Mutation Project | Wild type |
| *oac-36*(gk124636*)* | VC20551 | Million Mutation Project | Wild type |
| *oac-38*(*gk648702*) | VC40461 | Million Mutation Project | Reduced mbas#3 |
| *oac-39*(*gk145*) | VC247 | Deletion mutant from CGC | Wild type |
| *oac-4*(*gk363869*) | VC20633 | Million Mutation Project | Wild type |
| *oac-40*(*gk242459*) | VC20235 | Million Mutation Project | Wild type |
| *oac-41*(*gk242464*) | VC20211 | Million Mutation Project | Wild type |
| *oac-41*(*gk766757*) | VC40696 | Million Mutation Project | Wild type |
| *oac-42*(*WBVar00026105*) | CB4856 | Wild isolate | Wild type |
| *oac-43*(*gk737013*) | VC40638 | Million Mutation Project | Wild type |
| *oac-49*(*gk264009*) | VC20294 | Million Mutation Project | Wild type |
| *oac-5*(*gk398429*) | VC30020 | Million Mutation Project | Wild type |
| *oac-50*(*gk402144*) | VC20784 | Million Mutation Project | Reduced mbas#3 |
| *oac-51*(*gk533438*) | VC40246 | Million Mutation Project | Wild type |
| *oac-54*(*gk684785*) | VC40540 | Million Mutation Project | Wild type |
| *oac-6*(*gk735518*) | VC40635 | Million Mutation Project | Wild type |
| *oac-7*(*gk586689*) | VC40345 | Million Mutation Project | Wild type |
| *oac-8*(*gk211086*) | VC20046 | Million Mutation Project | Wild type |
| *oac-9*(*gk662463*) | VC40490 | Million Mutation Project | Wild type |

## 3.7 Materials and Methods

### *3.7.1 Maintenance of C. elegans Strains*

Wild type (N2, Bristol), GH10 *glo-1*(*zu437*), RB811 *glo-4*(*ok623*), RB662 *apb-3*(*ok429*), FX06781 *acs-7*(*tm6781*), GH378 *pgp-2(kx48)*, and PS7396 *acs-7(tm6781);syIs459[Pacs-7::ACS-7::GFP::unc-54 3'UTR*, 10 ng/μL; *Pmyo-2::dsRed*, 5 ng/μL] strains were maintained on NGM plates with *Escherichia coli* OP50 as the food source at room temperature as originally described, unless otherwise stated.[25] Some strains were obtained from the Caenorhabditis Genetics Center (CGC, USA) and the National BioResource Project (NBRP, Japan). GH10 was provided by D. Gems and *daf-22*(*ok693*) was a gift from H.Y. Mak. A list of *O*-acyltransferase mutants can be seen in Table 3.1. FCS10 *acs-7*(*tm6781*) was obtained by outcrossing FX06781 10x against GE1710 *rol-6*(*e187*); *unc-4*(*e120*). FCS10 was used for all experiments reported for *acs-7*(*tm6781*).

### *3.7.2 Molecular Biology*

Plasmids were constructed using standard molecular cloning techniques and Gibson Assembly (New England BioLabs, USA). To construct the *Pacs-7::ACS-7::gfp* rescue construct, pAEA10, the native *acs-7* promoter was PCR amplified from genomic DNA using 5' primer oAA065 and 3' primer oAA066 (see Appendix C) and inserted between FseI and AscI sites of pPH92, a gift from the Bargmann Lab. The cDNA sequence of the *acs-7* gene was amplified from plasmid pU57 provided by H. H. Le using 5' primer oAA067 and 3' primer oAA068 and inserted between AgeI and NheI sites upstream of the GFP coding region.

To assemble the *Pvha-6::mCherrySKL* peroxisomal marker construct, pAEA15, the mCherry coding sequence was PCR amplified from pPH93, a gift from the Bargmann Lab, using the 5' primer oAA093 and the 3' primer oAA094 which contains a nine nucleotide sequence encoding the SKL peroxisomal tag.[26] The fragment was then inserted between XmaI and KpnI sites of plasmid HYM433, kindly donated by H.Y. Mak.[15] The mCherrySKL sequence was placed downstream of the *vha-6* promoter and upstream of the 3'UTR region of the *unc-54* gene.

### *3.7.3 Transformation*

For *acs-7* rescue experiments, a DNA mixture of 10 ng/μL of pAEA10, 5 ng/μL of a *Pmyo-2::dsRed* co-injection marker, and 85 ng/μL of 1 kb ladder (New England BioLabs, USA) were injected into adult gonads of *acs*-7(*tm6781*) hermaphrodites using standard microinjection techniques.[27] Extrachromosomal arrays were then integrated into the genome via X-ray irradiation and integrants were outcrossed ten times with wild type strain N2 to create strain PS7396. For *acs-7* localization experiments, a DNA mixture of 30 ng/μL pAEA10 rescue construct, 30 ng/μL pAEA15, and 30 ng/μL *unc-119*(+) rescue construct were injected into adult gonads of PS6018 *unc-119*(*ed4*) hermaphrodites.[28]

### *3.7.4 CRISPR Knockout of acs-10*

An *acs-10* knockout mutant was created using the CRISPR/Cas9 genome editing system as previously described by Arribere *et al*.[29] Guide RNA (gRNA) templates were generated for four different binding sites within the *acs-10* gene by ligating corresponding

5’ and 3’ primers at the BsaI restriction site within the pRB1017 gRNA expression cassette vector provided by the Fire Lab (Stanford). For binding site 1, pAEA5 was generated using 5’ primer oAA001 and 3’ primer oAA002. For binding site 2, pAEA6 was generated using 5’ primer oAA003 and 3’ primer oAA004. For binding site 3, pAEA7 was generated using 5’ primer oAA005 and 3’ primer oAA006. For binding site 4, pAEA8 was created using 5’ primer oAA007 and 3’ primer oAA008.

A mixture of gRNA templates pAEA5, pAEA6, pAEA7, and pAEA8 (25 ng/μL each), plasmid pJA58 containing a gRNA directed at the gene *dpy-10* (25 ng/μL), a plasmid encoding *Peft-3::cas9* (Addgene #46168, 50 ng/μL), and the roller *dpy-10* repair oligo oHW36f (500 nM/μL) was injected into the adult gonad of wild type N2 hermaphrodite worms. Isolated injected animals were grown at room temperature and F1 progeny of the roller phenotype were selected and individually plated. After three days, plates were screened for F2 progeny displaying a roller phenotype, signaling likely co-conversion CRISPR positive plates.

Worms from each potentially CRISPR positive plate were lysed in 2.5 μL of worm lysis buffer supplemented with 0.5 mg/mL Proteinase K and genotyped by PCR using primer oAA009 and primer oAA010. PCR products were analyzed by gel electrophoresis and bands of shorter length than the predicted product were excised and send for DNA sequencing to confirm a deletion. F2 progeny from those plates were individually plated to isolate a homozygote of the deletion mutant.

### *3.7.5 Nematode Culture and Extraction*

Worms of mixed stages were washed from a 10 cm NGM agar plate seeded with *E. coli* OP50 into 25 mL of S-complete medium. Cultures were grown for 7 days at 22°C while shaking at 220 rpm for 7 days. Cultures were fed *E. coli* OP50 on days 1, 3, and 5. On day 7, cultures were centrifuged and worm pellets and supernatant were frozen separately, lyophilized, and extracted with 35 mL of 95% ethanol at room temperature for 12 hours. The extracts were dried *in vacuo*, resuspended in 200 μL of methanol and analyzed by HPLC-MS. All cultures were grown in at least two biological replicates.

### *3.7.6 Mass Spectrometric Analysis*

High resolution HPLC-MS analysis was performed on a Dionex 3000 UPLC coupled with a Thermo Q Exactive high-resolution mass spectrometer as described previously.[30] Metabolites were separated using a water-acetonitrile gradient on an Agilent Zorbax Eclipse XDB-C18 column (150 mm x 2.1 mm, particle size 1.8 μm) maintained at 40°C. Solvent A: 0.1% formic acid in water; Solvent B: 0.1% formic acid in acetonitrile. A/B gradient started at 5% B for 5 minutes after injection and increased linearly to 100% B at 12.5 minutes. Most ascarosides were detected as $[M-H]^-$ ions or $[M-Cl]^-$ adducts in the negative ionization mode (spray voltage 3 kV) and confirmed based on their high-resolution masses (<1 ppm), fragmentation spectra, and comparison of retention times with those of synthetic standards.

Low resolution HPLC-MS was performed using the Agilent 1100 Series HPLC system equipped with an Agilent Eclipse XDB-C18 column (250 mm x 9.4 mm, particle size 5 μm), connected to a Quattro II or Quattro Ultima mass spectrometer.[13] Solvent A: 0.1%

acetic acid in water; Solvent B: 0.1% acetic acid in acetonitrile. A/B gradient started at 5% B for 5 minutes after injection and increased linearly to 100% B over a period of 40 minutes. Ascarosides were detected as $[M-H]^-$ ions in the negative ionization mode (spray voltage 3.5 kV, cone voltage -40 V) and confirmed based on comparison of retention times with those of synthetic standards.

### *3.7.7 Microscopy*

LysoTracker staining was performed as previously reported by Hermann *et al*.[23] A 1 mM stock solution of LysoTracker Red (Thermo Fisher, USA) was diluted to 2 μM in M9 buffer, of which 0.5 mL was added to an NGM plate seeded with *E. coli* OP50 and incubated overnight at 20°C. Worms were added to the plate and grown overnight in the dark.

For imaging, worms were removed from the plate and transferred onto a glass slide with a thin 2% agarose pad containing 5 mM levamisole. Microscopic analysis was performed with a wide-field epifluorescence Zeiss Axioskop microscope equipped with a 100x oil objective. Images were taken with a Hamamatsu ORCA-ER digital camera using Openlab imaging software.

## 3.8 References


1. Jeong, P. Y.; Jung, M.; Yim, Y. H.; Kim, H.; Park, M.; Hong, E.; Lee, W.; Kim, Y. H.; Kim, K.; Paik, Y. K., Chemical structure and biological activity of the Caenorhabditis elegans dauer-inducing pheromone. *Nature* **2005,** *433* (7025), 541-5.
2. Butcher, R. A.; Fujita, M.; Schroeder, F. C.; Clardy, J., Small-molecule pheromones that control dauer development in Caenorhabditis elegans. *Nat Chem Biol* **2007,** *3* (7), 420-2.
3. Butcher, R. A.; Ragains, J. R.; Kim, E.; Clardy, J., A potent dauer pheromone component in Caenorhabditis elegans that acts synergistically with other components. *Proc Natl Acad Sci U S A* **2008,** *105* (38), 14288-92.
4. Srinivasan, J.; Kaplan, F.; Ajredini, R.; Zachariah, C.; Alborn, H. T.; Teal, P. E.; Malik, R. U.; Edison, A. S.; Sternberg, P. W.; Schroeder, F. C., A blend of small molecules regulates both mating and development in Caenorhabditis elegans. *Nature* **2008,** *454* (7208), 1115-8.
5. Pungaliya, C.; Srinivasan, J.; Fox, B. W.; Malik, R. U.; Ludewig, A. H.; Sternberg, P. W.; Schroeder, F. C., A shortcut to identifying small molecule signals that regulate behavior and development in Caenorhabditis elegans. *Proc Natl Acad Sci U S A* **2009,** *106* (19), 7708-13.
6. Ren, P.; Lim, C. S.; Johnsen, R.; Albert, P. S.; Pilgrim, D.; Riddle, D. L., Control of C. elegans larval development by neuronal expression of a TGF-beta homolog. *Science* **1996,** *274* (5291), 1389-91.

7. Kimura, K. D.; Tissenbaum, H. A.; Liu, Y.; Ruvkun, G., daf-2, an insulin receptor-like gene that regulates longevity and diapause in Caenorhabditis elegans. *Science* **1997,** *277* (5328), 942-6.

8. Srinivasan, J.; von Reuss, S. H.; Bose, N.; Zaslaver, A.; Mahanti, P.; Ho, M. C.; O'Doherty, O. G.; Edison, A. S.; Sternberg, P. W.; Schroeder, F. C., A modular library of small molecule signals regulates social behaviors in Caenorhabditis elegans. *PLoS Biol* **2012,** *10* (1), e1001237.

9. Artyukhin, A. B.; Yim, J. J.; Srinivasan, J.; Izrayelit, Y.; Bose, N.; von Reuss, S. H.; Jo, Y.; Jordan, J. M.; Baugh, L. R.; Cheong, M.; Sternberg, P. W.; Avery, L.; Schroeder, F. C., Succinylated octopamine ascarosides and a new pathway of biogenic amine metabolism in Caenorhabditis elegans. *J Biol Chem* **2013,** *288* (26), 18778-83.

10. Walsh, C. T., The chemical versatility of natural-product assembly lines. *Acc Chem Res* **2008,** *41* (1), 4-10.

11. Meier, J. L.; Burkart, M. D., The chemical biology of modular biosynthetic enzymes. *Chem Soc Rev* **2009,** *38* (7), 2012-45.

12. Edison, A. S., Caenorhabditis elegans pheromones regulate multiple complex behaviors. *Curr Opin Neurobiol* **2009,** *19* (4), 378-88.

13. von Reuss, S. H.; Bose, N.; Srinivasan, J.; Yim, J. J.; Judkins, J. C.; Sternberg, P. W.; Schroeder, F. C., Comparative metabolomics reveals biogenesis of ascarosides, a modular library of small-molecule signals in C. elegans. *J Am Chem Soc* **2012,** *134* (3), 1817-24.

14. Izrayelit, Y.; Srinivasan, J.; Campbell, S. L.; Jo, Y.; von Reuss, S. H.; Genoff, M. C.; Sternberg, P. W.; Schroeder, F. C., Targeted metabolomics reveals a male pheromone and sex-specific ascaroside biosynthesis in Caenorhabditis elegans. *ACS Chem Biol* **2012,** *7* (8), 1321-5.

15. Butcher, R. A.; Ragains, J. R.; Li, W.; Ruvkun, G.; Clardy, J.; Mak, H. Y., Biosynthesis of the Caenorhabditis elegans dauer pheromone. *Proc Natl Acad Sci U S A* **2009,** *106* (6), 1875-9.

16. Izrayelit, Y.; Robinette, S. L.; Bose, N.; von Reuss, S. H.; Schroeder, F. C., 2D NMR-based metabolomics uncovers interactions between conserved biochemical pathways in the model organism Caenorhabditis elegans. *ACS Chem Biol* **2013,** *8* (2), 314-9.

17. Zhang, X.; Feng, L.; Chinta, S.; Singh, P.; Wang, Y.; Nunnery, J. K.; Butcher, R. A., Acyl-CoA oxidase complexes control the chemical message produced by Caenorhabditis elegans. *Proc Natl Acad Sci U S A* **2015,** *112* (13), 3955-60.

18. Moerman, D. G., Strasbourger, P., Thompson, O., Adair, R., Au, V., Chaudhry, I., Edgley, M., Ewing, B., Fernando, L., Flibotte, S., High, A., Hillier, L., Hutter, H., Lau, J., Lee, N., Miller, A., Raymant, G., Shendure, J., Taylor, J., Turner, E.H., Waterston, R. , The million mutation project a genetic resource for C. elegans. *Worm Breeder's Gazette* **2012,** *19.2* (3).

19. Gould, S. J.; Keller, G. A.; Hosken, N.; Wilkinson, J.; Subramani, S., A conserved tripeptide sorts proteins to peroxisomes. *J Cell Biol* **1989,** *108* (5), 1657-64.

20. Panda, O.; Akagi, A. E.; Artyukhin, A. B.; Judkins, J. C.; Le, H. H.; Mahanti, P.; Cohen, S. M.; Sternberg, P. W.; Schroeder, F. C., Biosynthesis of Modular Ascarosides in C. elegans. *Angew Chem Int Ed Engl* **2017,** *56* (17), 4729-4733.

21. Chitwood, B. G.; Chitwood, M. B. H., *Introduction to nematology*. Consolidated ed.; University Park Press: Baltimore,, 1974; p 334 p.

22. Laufer, J. S.; Bazzicalupo, P.; Wood, W. B., Segregation of developmental potential in early embryos of Caenorhabditis elegans. *Cell* **1980,** *19* (3), 569-77.

23. Hermann, G. J.; Schroeder, L. K.; Hieb, C. A.; Kershner, A. M.; Rabbitts, B. M.; Fonarev, P.; Grant, B. D.; Priess, J. R., Genetic analysis of lysosomal trafficking in Caenorhabditis elegans. *Mol Biol Cell* **2005,** *16* (7), 3273-88.

24. Mony, V. K.; Benjamin, S.; O'Rourke, E. J., A lysosome-centered view of nutrient homeostasis. *Autophagy* **2016,** *12* (4), 619-31.

25. Brenner, S., The genetics of Caenorhabditis elegans. *Genetics* **1974,** *77* (1), 71-94.

26. Thieringer, H.; Moellers, B.; Dodt, G.; Kunau, W. H.; Driscoll, M., Modeling human peroxisome biogenesis disorders in the nematode Caenorhabditis elegans. *J Cell Sci* **2003,** *116* (Pt 9), 1797-804.

27. Mello, C. C.; Kramer, J. M.; Stinchcomb, D.; Ambros, V., Efficient gene transfer in C.elegans: extrachromosomal maintenance and integration of transforming sequences. *EMBO J* **1991,** *10* (12), 3959-70.

28. Maduro, M.; Pilgrim, D., Identification and cloning of unc-119, a gene expressed in the Caenorhabditis elegans nervous system. *Genetics* **1995,** *141* (3), 977-88.

29. Arribere, J. A.; Bell, R. T.; Fu, B. X.; Artiles, K. L.; Hartman, P. S.; Fire, A. Z., Efficient marker-free recovery of custom genetic modifications with CRISPR/Cas9 in Caenorhabditis elegans. *Genetics* **2014,** *198* (3), 837-46.

30. Markov, G. V.; Meyer, J. M.; Panda, O.; Artyukhin, A. B.; Claassen, M.; Witte, H.; Schroeder, F. C.; Sommer, R. J., Functional Conservation and Divergence of daf-22 Paralogs in Pristionchus pacificus Dauer Development. *Mol Biol Evol* **2016,** *33* (10), 2506-14.